Power Optimization in Hybrid Renewable Energy Standalone System using SMC-ANFIS

Viswanathan KALVINATHAN[1], Subramanian CHITRA[2]
[1]*Department of Electrical and Electronics Engineering, Suguna College of Engineering, Coimbatore,Tamilnadu, India - 641014*
[2]*Department of Electrical and Electronics Engineering, Government College of Technology, Coimbatore,Tamilnadu, India - 641013*
kalvinathan@sugunace.com

***Abstract*—The integration of renewable energy sources is challenging now-a-days because of intermittent nature of solar radiation. Particularly in hybrid renewable energy system, it is required to incorporate an intelligent control algorithm to optimize the time duration at transient condition and also ensures the stable operation. This paper is aimed at integrating hybrid renewable energy system includes partial shaded solar photovoltaic system and Proton Exchange Membrane Fuel Cell (PEMFC) at constant temperature to supply the stand-alone DC load. Due to the dynamic DC source, an Energy Management System (EMS) is used to get the stable output. The system includes interleaving soft switching boost converters (SSBC's) is controlled by combined Slide Mode Controller with trained Artificial Neuro Fuzzy System (SMC-ANFIS). The proposed Hybrid system is modeled and simulated using MATLAB Simulink platform. The tested parameters are obtained in terms of voltage, current, power, speed, and torque. The simulated result of proposed system with SMC-ANFIS-EMS is compared with conventional SMC-EMS and SMC-ANN-EMS to obtain optimal output. From the performance analysis, the SMC-ANFIS-EMS provides better output and control.**

***Index Terms*—performance analysis, hybrid system, power management, photo voltaic, fuel cell.**

I. INTRODUCTION

In recent years, due to increased population, the demand for electricity seems to be increasing across the globe. On the other side, the availability of fossil fuels is reducing, and usage of conventional sources leads to create adverse environmental impacts. To compensate energy demand and maintain pollution free environment, the need for alternative energy resources is becoming essential. The solar energy, fuel cell and wind are the cheapest renewable energy sources that can be easily converted into electrical energy. Solar power can be extracted only during shiny time of day, probably it holds up to eight hours of daytime. A well-designed Energy storage system can help electrical grid to provide good balance between sources and load during dynamic condition. The solar energy can be easily convert into electricity and also the PEMFC plays significant role in power generation. However, the solar resource always in dynamic and hence the storage system is provided with solar PV system for stable operation. The hybrid model of PV and PEMFC standalone system can be utilized in remote areas where difficult to provide electricity. The solar PV has the advantage of long life time and pollution free power generation [1-4]. The integration of various renewable resources such as PV, wind, diesel for small distribution system and its feasibility are analysed. The small scale distribution system has the advantage of less transmission loss, increased reliability and better control. Based on the analysis, an optimum configuration is needed for the intermittent service and also addition of batteries and FC's to dynamic renewable resources will improve the reliability of the stand-alone-system [5-7]. The renewable energy (REs) is efficiently interfaced with low-voltage DC microgrid. The introduction of bipolarity in DC microgrid will increase the reliability of the network. The energy storage system is always associated with hybrid REs because of its uncertainties. The storage system may increase the total cost microgrid, also need of optimal sizing and siting of REs which will increase the complexity in optimization. A study on PV integrated with Fuel Cell is carried out instead of batteries as back up source. An optimal PV and FC based microgrid is investigated with considering reliability and economic costs under the limitations of system operation [8-13]. In a hybrid renewable energy system, an effective control algorithm has to be developed to optimize the system. An intelligent fuzzy logic controller regulates the DC grid voltage with quick response and improves stabilization problems in the power system. Model predictive controls (MPC) optimize the resource scheduling, minimize the operating cost and energy storage system degradation. The islanded micro grid with MPC and fuzzy based EMS are investigated. The effectiveness of the microgrid power system can be improved by a suitable energy management schemes [14-16]. A strategy is required for hybrid power system to manage the power fluctuations among the sources and load power. The Power Management Strategy (PMS) manage the sources effectively and also improves life cycle of chargeable storage equipment. A Particle Swarm Optimization (PSO) algorithm is implemented for an islanded PV model to reduce the variation in power and frequency level [17-20]. The Maximum Power Point Tracking (MPPT) methods can improve the performance of hybrid system. An intelligent method developed for MPP tracking based on adaptive neuro fuzzy inference system. During transient conditions, there is a variation in power and frequency in islanded mode. A fuzzy controlled energy management unit (EMU) is designed with an effective control strategy to integrate with utility grid [21-25].

Digital Object Identifier 10.4316/AECE.2022.03008

From the detailed analysis of literature, there is a need to control the power flow among the sources and load for Hybrid Renewable Energy stand alone system. Many literatures are analysed with different control algorithm such as MPPT, ANN, Fuzzy, MPO etc., Hence an intelligent control algorithm is required with hybrid system to manage the power fluctuations during the switching of the renewable sources. The EMS should optimize the time duration at transient condition and provide uninterrupted power supply to the load.

II. Proposed Methodology

The proposed system consists of partially shaded photo voltaic (PV) array and Fuel cell (FC) system as shown in Fig. 1. The Renewable source is link with DC bus through DC interleaved boost converter (ISSBC) and supplies power to PMDC motor.

In this work, SMC-ANFIS-EMS is modelled with partial shaded PV and fuel cell hybrid standalone system under MATLAB Simulink environment.

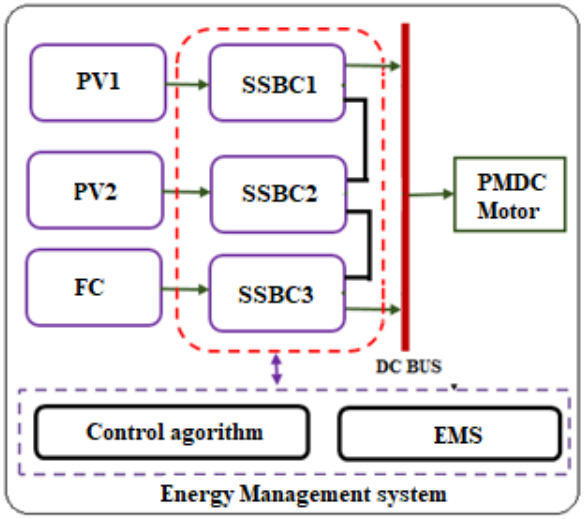

Figure 1. System configuration

III. System Modeling

A. Photo Voltaic Array

The DC-DC conversion of the PV system has two panels connected in series. It is rated for Power of 315 W with operating voltage of 37.28 V, current of 8.45 A at standard test condition. Each PV cell is modelled with a single-diode, connected with series and shunt resistance whose equivalent circuit is shown in Fig. 2.

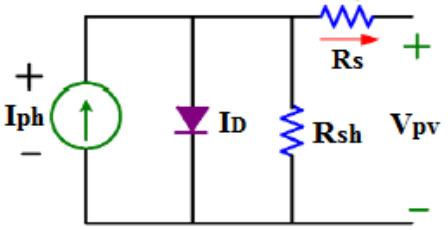

Figure 2. Equivalent circuit

The power ratings of SPV panel are taken from PV module manufacture datasheet, which is shown in Table I. The PV model is implemented in MATLAB Simulink tool by using the basic circuit equation (1)

$$I_{pv} = I_0\left[\exp\left(\frac{qV_{0c}}{A_i kT} - 1\right)\right] - \frac{V + IR_s}{R_{sh}} \quad (1)$$

TABLE I. PV PARAMETERS

Parameters	Values
Panel Short-Circuit Current (I_{SC})	8.95
Panel Open-Circuit Voltage(V_{OC})	45.22
Maximum Current (I_{mp})	8.45
Maximum Voltage (V_{mp})	37.28
Maximum Power(P_{max})	315
Number of series cells	10

The Table I shows the modelled panel specifications. The maximum voltage at no-load (V_{oc}) is about 45.22 V and Short-circuit current (I_{sc}) is 8.95 A. The PV parameters are expressed as Solar irradiation (λ_i) (W/m^2), charge quantity (q), Diode ideality factor (A_i), Boltzmann's constant (k), Light energy conversion from current (I_{ph}), short-circuit current (I_{sc}), saturation current (I_o), Reverse saturation current (I_{rs}) and PV current (I_{pv}).

The power is extracted from the panel when operating at Standard Testing Conditions parameters of panel insolation of 1000 W/m^2 at temperature 25 ^{0}C.

The obtained I-V and P-V characteristics curves from simulation are shown in the Fig. 3. The curves obtained are exactly match with the experimental datasheet. Fig. 3 shows the different insolation (1000 W/m^2, 500 W/m^2 and 100 W/m^2) characteristics of the 315 kW of the PV system.

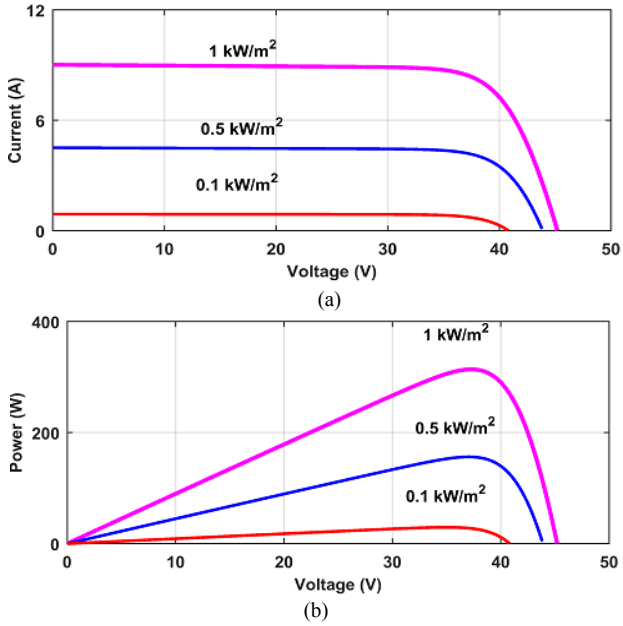

Figure 3. (a) I-V, (b) P-V characteristics

B. Shaded PV System Model

Partial shading of solar PV results is also tested for different radiations. The equation (2) and (3) is given by the partially shaded model of a PV module with N series cells.

The PV array cells connected to the series and parallel configuration based on rated load power. In the partially shading condition more power draw and create junction temperature at that duration lead to create a hotpot in PV modules.

In order to avoid hotpot problem to insert bypass diode across PV module but bypass diode leads to multiple peaks means local maxima in PV panel characteristics. In this condition to find the global peak (GP) from many local

peaks is a real challenge for extract maximum power intelligence PMS method.

$$I_{pv}=\begin{cases} I_{ph}(G_1)-I_{01}\left[exp\left(\frac{q(V_{pvm1}+I_{pv}R_{se})}{N_sAkT_k}\right)-1\right]-\frac{(V_{pvm1}+I_{pv}R_{se}N_s)}{R_pN_s} & I_{pv}>I_{ph1} \\ I_{ph}(G_2)-I_{01}\left[exp\left(\frac{q(V_{pvm2}+I_{pv}R_{se})}{N_sAkT_k}\right)-1\right]-\frac{(V_{pvm2}+I_{pv}R_{se}N_s)}{R_pN_s} & I_{pv}<I_{ph2} \end{cases} \quad (2)$$

$$V_{pv}=\begin{cases} V_{pv1}I_{pv} > I_{ph1} \\ V_{pv2}+V_{pv1}I_{pv} < I_{ph2} \end{cases} \quad (3)$$

The developed simulation model series connected two partial shaded PV panel I-V and P-V characteristics shown in the Fig. 4. From observation of the Fig. 4 gives the inflexion point 'I' is the intersection of the P-V characteristic of P-V response of shaded photovoltaic generation.

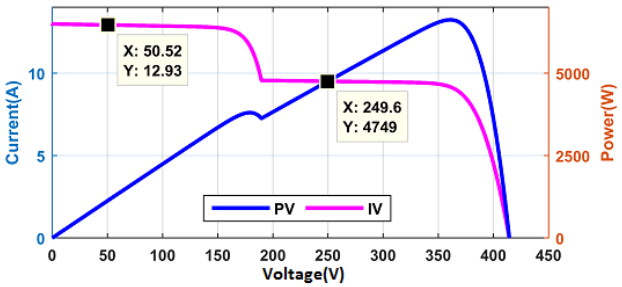

Figure 4. P-V and I-V characteristics PV panel

C. Fuel Cell (FC)

The FC power is converted to the appropriate voltage by the ISSBC conversion system using the electrolyze process; it splits the water into hydrogen and oxygen. The hydrogen is a fuel, so it is stored as hydrogen (H_2) fuel stock and fed back to the fuel cell again. The operating parameter of fuel cell stack power is 6 kW, 133.3 A, with fuel flow of 50.06 (lpm), at operating temperature of 338 kelvin as shown in Table II.

TABLE II. FC SPECIFICATION

Parameters	Rated Values
Stack Power	6000W
Nominal Voltage	45V
Nominal current	133.3A
Number of cell	65
Operation temperature	338 kelvin
Air flow rate	300 lpm
Fuel flow rate	50.06 lpm

$$H_2+\frac{1}{2}O_2 \rightarrow H_2O+Heat+ElectricalEnergy \quad (4)$$

The detailed PEMFC model selected from MATLAB/Simulink and it is integrated into the PV system. The fuel cell is developed as controlled voltage source and its model is shown in Fig. 5.

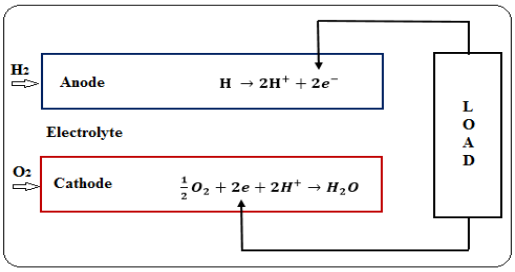

Figure 5. Cross-sectional view of PEMFC

D. DC-DC Converter

The ISSBC converter is connected with PV1, PV2 array and FC system for power conversion (low voltage high current into a high voltage low current output system). The ISSBC consists two single boost converter that are connected and operating 180^0 out of phase with 10 kHz switching frequency to extract maximum power from PVs and FC systemand modulation index are defined by the equation (5) to (8)

$$V_o=V_{pv}\left(\frac{1}{2}(1-D)\right) \quad (5)$$

$$V_o=\frac{1}{2}\left(\frac{1}{1-D}\right)V_{pv} \quad (6)$$

$$I_o=\frac{1}{2}\left(\frac{1}{1-D}\right)I_{pv} \quad (7)$$

$$M=\frac{1}{2}\left(\frac{1}{1-D}\right)=\frac{V_o}{V_{pv}} \quad (8)$$

where, V_o - output voltage, V_{pv} - input voltage, D - duty cycle, I_{pv} - input current, I_o - output current, M - Modulation Index.

TABLE III. CONVERTER SIMULATION PARAMETERS

Parameters	Value
The RMS line voltage of the AC load	600 V
Pulse switching Frequency	10 kHz
DC capacitor voltage	897 V
Capacitance	2200 µF
The carrier sub-bands	h1 = 0.8, h2 = 0.2

The parameters of DC-DC converter is shown in Table III. The simulation results are obtained for the various operating conditions likely dynamic load. The output results are analyzed to obtain optimal operating parameters. The obtained parameters can be used for the further analysis.

IV. POWER MANAGEMENT CIRCUIT

The proposed EMC controller algorithm implement the by the logical switching (ON and OFF) simulation block sets. The controller observes the PV and FC power and compare with the load if demand less then PV power the excess power sent to storage device. The load demand more than PV system the required power supplies from FC stack. The switching mechanism for SMC-ANFIS-EMS system mentioned is in Fig. 6.

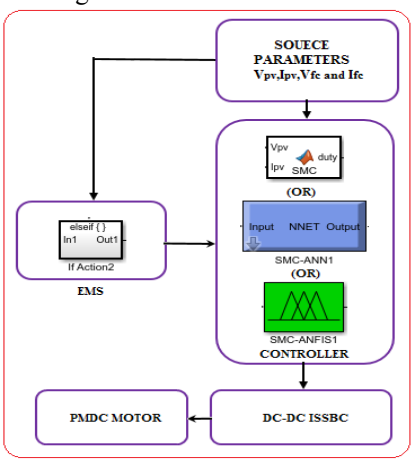

Figure 6(a). Circuit diagram of EMC system

A. SMC Algorithm

The SMC controller extracts the MPPT PV and FC system with quick energetic response as shown in Fig. 7.

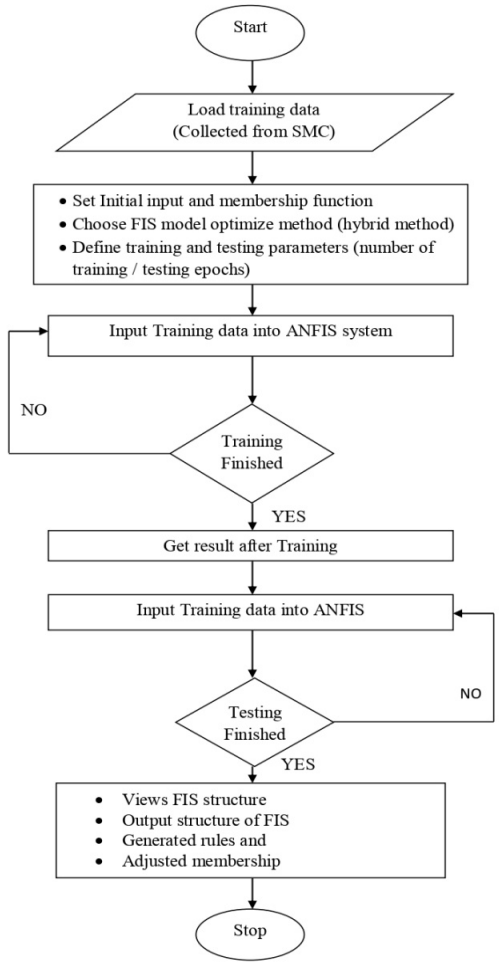

Figure 6(b). Flow Chart of EMC system

The controller operating instruction from the energy management system (EMS) is based on the available source voltage (V_s) and source current (I_s) as well as output produced by the duty cycle of modulation index (MI). The system is implemented and developed in the 'IF' and 'ELSE' simulink blocks. The system is operated by conditional power availability of the PV1, PV2 and FC renewable system. The sliding surface 'Ψ' and 'Φ' is chosen to extract the MPPT location from the PV array and FC power conversion system.

$$\psi = \frac{\partial P_{pv}}{\partial I_{pv}} and \varphi = \frac{\partial P_{FC}}{\partial I_{FC}} \tag{9}$$

where, P_{pv} – power availability of PV system, P_{FC} – Power availability of Fuel Cell, I_{FC} – Current of Fuel Cell.

The PV power sensed and P_{pv} and P_{FC} is found as,

$$P_{pv} = V_{pv} I_{pv} and P_{FC} = V_{FC} I_{FC} \tag{10}$$

Taking the derivative of equation (10) as,

$$\frac{\partial P_{pv}}{\partial I_{pv}} = V_{pv} + I_{pv} \frac{\partial V_p}{\partial I_p} and \frac{\partial P_{FC}}{\partial I_{FC}} = V_{FC} + I_{FC} \frac{\partial V_{FC}}{\partial I_{FC}} \tag{11}$$

Sliding surface calculated by equation (11) as,

$$\psi = V_{pv} + I_{pv} \frac{\partial V_p}{\partial I_p} and \psi = V_{FC} + I_{FC} \frac{\partial V_{FC}}{\partial I_{FC}} \tag{12}$$

To solve the equation (9)-(12) is set to zero. SMC can be defined as,

$$d = \upsilon + ksign(\psi) \; and \; d = \upsilon + ksign(\varphi) \tag{13}$$

where, k - gain constant, υ - equivalent control. The υ is obtained as,

$$\upsilon = 1 - \frac{V_{pv}}{V_{dc}} and \upsilon = 1 - \frac{V_{FC}}{V_{dc}} \tag{14}$$

the duty cycle d differs between 0 and 1. Hence the SMC logic distinct as,

$$d = \begin{cases} 1; if \; \upsilon + ksign(\psi) > 0 \\ 0; if \; \upsilon + ksign(\psi) < 0 \end{cases}, d = \begin{cases} 1; if \; \upsilon + ksign(\varphi) > 0 \\ 0; if \; \upsilon + ksign(\varphi) < 0 \end{cases} \tag{15}$$

The SMC program script is embedded in the user definition function as Simulink block. The modulation index is initiated to the PWM generator with frequency of 5000 kHz with damping factor constant of 1074. The generated pulses are used to control the ISSB converter. Optimal operation of SMC controller appropriates the operational conditions of the PV and FC system.

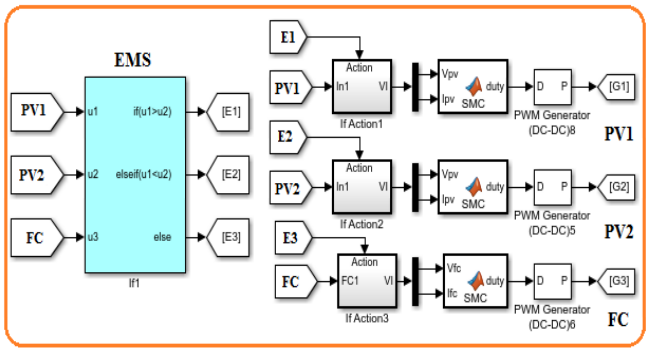

Figure 7. SMC-EMS

B. *SMC - ANN*

The ANN algorithm operates like a human brain and attempts to imitate the method of learning. The ANN is trained with 5000 input and the output data is extracted from the SMC-EMC controller. The trained block replaces the conventional SMC controller as shown in Fig. 8. The ANN is input output pattern matching intelligent controller system. The output performance obtained mean-square error as shown in Equation (16).

$$e = \frac{1}{p} \sum_{i=1}^{p} \left\| y^{(i)} - v^{(i)} \right\|^2 \tag{16}$$

where, p = training datas, y = SMC-ANN response vector, v = desired output.

$$a_j = \tan sig\left(\sum_{k=1}^{n} w_k v_k + bias \right) \tag{17}$$

'w_k' - synapse weight linked of each 'n' inputs.

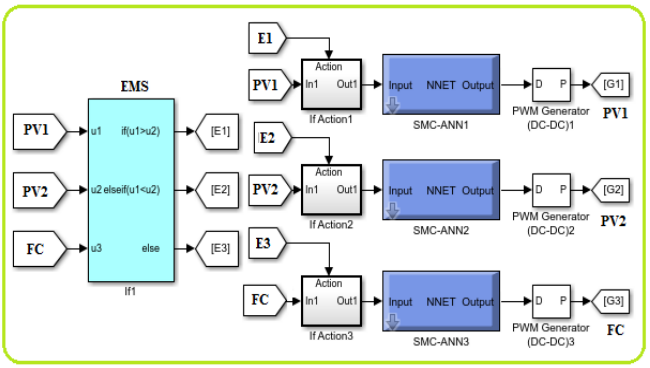

Figure 8. SMC-ANN-EMS

In Equation 17, the sigmoid function of the consequential prejudiced sum plus bias connected will be measured as an added input produces the output. The output of ANN block will produce modulation index (MI) and pulse is generated

using PWM generator and that ignites the energy conversion system.

C. SMC - ANFIS

The ANFIS controller combination of the FLC-ANN powerful tool used to control and optimize the performance of composite system including nonlinear response of PV and FC systems. ANN functions of statistics training, while FLC are based on skilled knowledge. ANFIS builds input output mapping on generated input output data pair by using least squares and back propagation gradient method. The fuzzy if-then rules of the Sugeno fuzzy system are given as follows:

$$Rule\,1: if X(t-1) is A_1 and Y(t) is B_1, then F_1 = m\,X(t) n_1 Y + k_1 \quad (18)$$

$$Rule\,2: if X(t-1) is A_2 and Y(t) is B_2, then F_2 = m_1 X(t) n_1 Y + k_2 \quad (19)$$

The small letters "m', 'n', and 'k' of signify the linear parameters, the capital letters 'A' and 'Indicate are nonlinear parameters. In this first layer, the numerical data is converted to the fuzzy then the equations are defined as

$$Z_{1,j} = \mu_{Ai}(X)\, for i = 1,2 \quad (20)$$

$$Z_{1,j} = \mu_{Ai}(Y)\, for i = 3,4 \quad (21)$$

$Z_{1,j}$ - membership value X, and Y, 'μ' - membership function, i - node and j - layer numbers. In the second layer, the output is the product of every input response.

$$Z_{2,j} = \mu_{Ai}(X)\,\mu_{Bi}(Y) \quad (22)$$

This third layer of fuzzy system is found as

$$Z_{3,i} = \varpi_i = \frac{\omega_i}{\omega_1 + \omega_2} \quad (23)$$

'ϖ_i' - optimal firing strength. Function of fourth layer linguistic value is converted to numerical values

$$Z_{4,j} = \varpi = \varpi(p_i X + q_i Y + r_i)\, for i = 1,2 \quad (24)$$

'p_i', 'q_i', 'r_i' are consequent parameters. It calculates the overall output value

$$Z_{5,j} = \sum_i \varpi_i F_i = \frac{\sum_i \varpi_i F_i}{\sum_i \varpi_i} \quad (25)$$

Input variables to the ANFIS controller are PEMFC and PV parameters and the output is modulation index.

The data set is collected from SMC-EMC conventional system and trained by the ANFIS tool. The three different configurations contain 5000 input parameter of voltage, current and output parameter of corresponding modulation index and setting of 3000 epochs. From that dataset, ANFIS will generate a fuzzy inference system (FIS) data structure. The structure membership parameters are tuned, and the error (0.01%) is optimized by back propagation algorithm. The output response of surface view is shown in Fig. 9. The SMC-ANFIS-EMC of standalone hybrid system is developed and shown in Fig. 10.

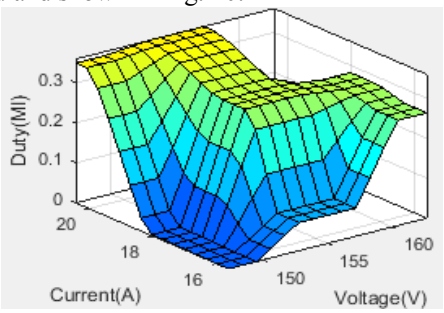

Figure 9. ANFIS surface view generated rules

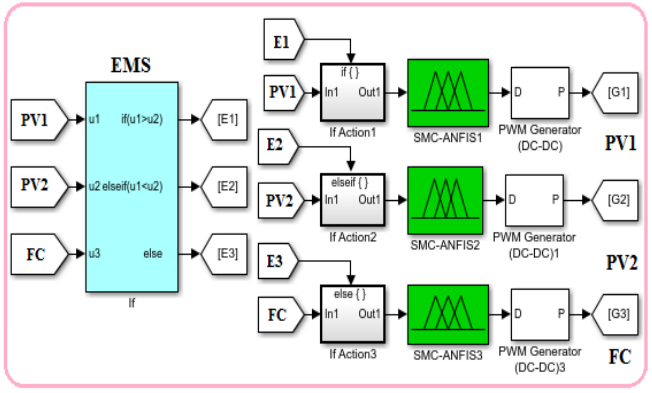

Figure 10. SMC-ANFIS-EMS

V. Simulation and Results

The performance of the different EMC-MPPT of hybrid PV and fuel cell's are controlled and overall simulation scheme is studied, and it is presented in Fig. 11. The two individual PV module and FC stack are connected individually with ISSB converter. These three converters are serially connected with PMDC motor. To achieve the performance of the system is tested under different operating conditions and it is evaluated and investigated by SMC, SMC-ANN and SMC-ANFIS controller developed in MATLAB/Simulink platform. The different electrical and mechanical parameters and conversion efficiency are analysed. The operating configuration parameters are shown in Table IV, and simulated result of insolation of PV and FC fuel flow rate are presented in Fig. 12. The simulation is carried out for the duration of from 0s to 0.5s at the PV2 irradiation of 400 W/m2 with cell temperature of 250 ^{0}C and FC fuel pressure is of 30.06 (lpm) at stack temperature of 3380 K.

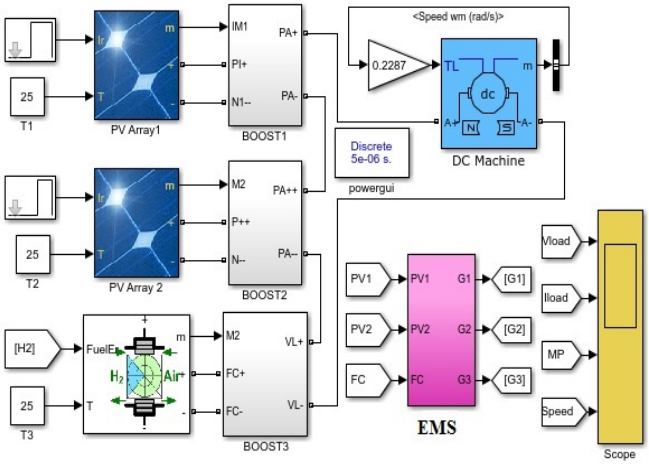

Figure 11. Simulation diagram of the system

The dynamic change is considered from 0.5s to 1s for the PV1 400 W/m^2 and PV2 600 W/m^2. During the period of 1s to 1.5s, irradiance of PV2 is of 450 W/m^2 and same fuel pressure for FC stack is considered. The interleaved converter mode with 60 kHz effect is developed by phase shifting of two 30 kHz switching signals. The dynamic change from one pattern to another should be analysed to accommodate the load mismatch with source. The load mismatch happens because of incident voltage drop and overshoots oscillations and it is managed by EMC control algorithm.

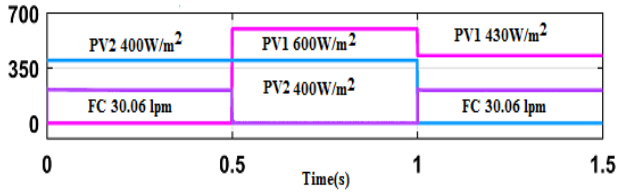

Figure 12. Insolation and fuel flow rate

TABLE IV. SIMULATION CONFIGURATION

Pattern	Time	Parameter		
		Insolation (W/m^2)(25^0C)		Fuel Pressure (lpm)(338K)
		PV1	PV2	FC
PT1	From (t=0.0s to t=0.5s)	-	400	30.06
PT2	From (t=0.5s to t=1.0s)	400	600	-
PT3	From (t=1.0s to t=1.5s)	-	450	30.06

In SMC-EMC controller, the PV and FC system characteristics are analyzed in terms of generated voltage, load voltage, load current, load power, motor speed and schedule time due to dynamical change from one pattern to another pattern is as shown in Fig. 13. It can be observed that the voltage variation of 159.10 at 400 W/m^2 (PV2) and FC voltage of 159.10 V at 30.06 (lpm) in the pattern 1 configuration. Similarly, there is a dynamical change in partial shaded condition in PT2 with transient voltage variation of 242.10 V with settling time of 0.5463s and 152.90 V with settling time of 0.548s respectively. In the Final pattern (PT3), PV2 produces transient voltage of 147.9 V with settling time 1.02s and 182 V with settling time 1.053s. Fuel cell produces 251.8 V at 1.022s and 210 V at 1.068s respectively.

The average power produced during different pattern is tabulated in Table V for SMC-EMC system. It is observed that, it produces 4760 W, 4710 W and 4880 W with oscillation of 5%, 3.31% and 1.3% respectively. The mechanical characteristics of torque and speed of SMC-EMC are shown in Table VI. In this observation torque oscillatory is about 20.10 Nm to 21.18 Nm and the speed of the motor varies from 767.50 rpm to 862.90 rpm respectively.

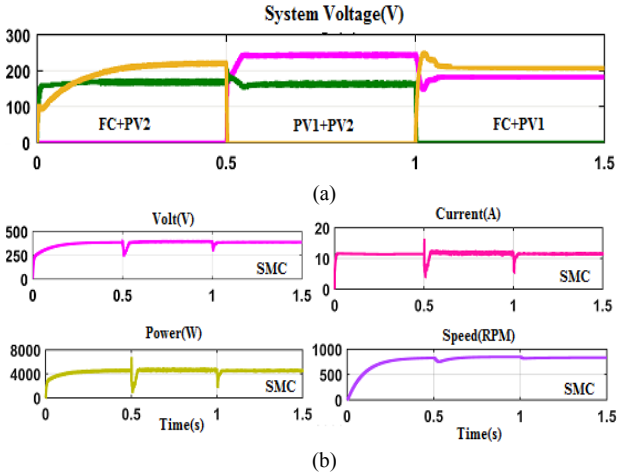

Figure 13. SMC-EMS: (a) Generated voltage, (b) Load Parameter

The same hybrid PV's with FC system is simulated for SMC-Artificial Neural Network based EMC with same patterns shown in Fig. 14. It is noted that in PT1, the generated voltage of 162.20 V at 400 W/m^2 (PV2) and FC voltage of 230.90 V at 30.06 (lpm). Similarly, there is a dynamical change in partial shaded condition in PT2 with transient voltage of 243.80 V with settling time of 0.520s and 160.60 V with settling time of 0.517s respectively. In the final PT3, PV2 produces transient voltage of 180.1 V with settling time 1.024s and 177 V with settling time 1.28sat 430 W/m^2. Fuel cell produces 255.10 V at 1.024s and 226.80 V at 1.028s respectively.

The average power produced during different patterns is tabulated in Table V for SMC-ANN-EMC system. It is observed that, it produces 4614 W, 4713 W and 4789 W with oscillations of 4.10% to 0.70%. The mechanical characteristics such as torque and speed of SMC-ANN-EMC are shown in Table VI. In this observation torque oscillatory is about 19.96 Nm to 21.02 Nm and the speed of the motor varies from 804.20 rpm to 861.90 rpm respectively.

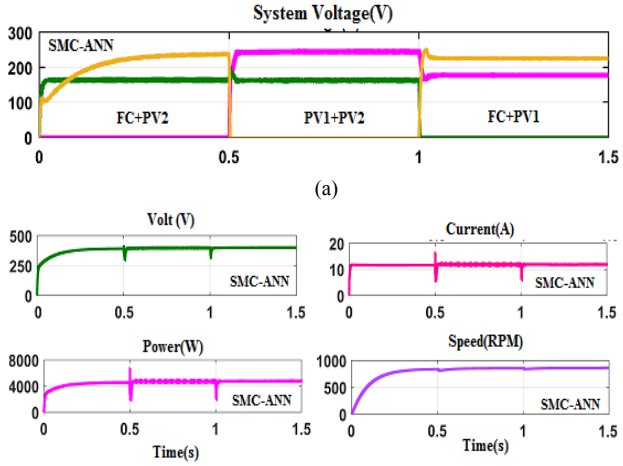

Figure 14. SMC-ANN-EMS: (a) Generated voltage, (b) Load Parameter

The same hybrid PVs with FC system is simulated for SMC-Artificial Neural Fuzzy Inference System based EMC with same patterns. It is noted that in PT1, the generated voltage of 161.50 V of (PV2) and 233.90 V of FC. Similarly, there is a dynamical change in partial shaded condition in PT2 with transient voltage of transient 242.10 V with settling time of 0.520s and 163.10 V with settling time of 0.517s. In the final PT3, PV2 produces transient voltage of 177.30 V with settling time 1.024s and 177.00 V with settling time 1.38s. Fuel Cell produces 221.70 V at 1.020s and 225.80 V at 1.028s respectively.

The average power produced during different patterns is tabulated in Table V for SMC-ANFIS-EMC system. It is observed that, it produces 4514 W, 4748 W and 4742 W with oscillatory 1.93% to 0.5%. The mechanical characteristics such as torque and speed of SMC-ANFIS-EMC are shown in Table VI. In this observation torque oscillatory is about 20.10 Nm to 20.98 Nm and its speed varies from 814.70 rpm to 859.40 rpm respectively.

A. Comparative Analysis

The Electrical and Mechanical parameters are tabulated in Table V and Table VI respectively for all EMC system. For PT1 configuration, in SMC-EMC, the voltage varies from maximum to minimum as 385.60 V to 366.60 V and the current varies from 12.98 A to 12.47 A and the power varies from 4826 W to 4695 W with oscillation 5.00%.

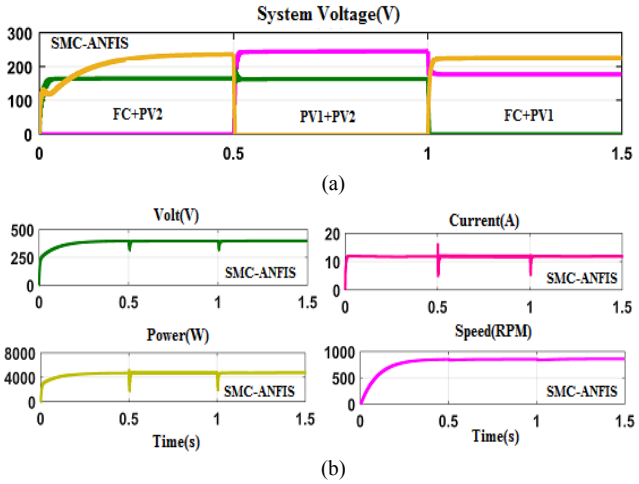

Figure 15. SMC-ANFIS-EMS: (a) Generated voltage, (b) Load parameter

In SMC-ANN the voltage varies from 390.50 V to 374.80 V and the current varies from 12.10 A to 11.53 A and the power varies from 4570 W to 4658 W with oscillation 4.10%. In SMC-ANFIS the voltage varies from 396.60 V to 393.00 V and the current varies from 11.80 A to 11.75 A and the power varies from 4531 W to 4497 W with oscillation 1.93%.

Specifically, the dynamical from PT1 to PT2 configuration for the period 0.5s to 1.0s, it's observed that the SMC-ANFIS has considerable response in all electrical and mechanical parameters compared to other two controllers such as SMC and SMC-ANN. The transient drop in power of SMC-EMS, SMC-ANN-EMS and SMC-ANFIS-EMS are 1444 W, 2008 W and 2029 W respectively.

The corresponding motor speed is 756.90 rpm, 849.30 rpm and 836.10 rpm. The power response of the SMC-ANFIS got the global peak power than other two controllers and the power has 1.5% to 0.3% less oscillatory.

TABLE V. SIMULATION RESULT OF ELECTRICAL PARAMETERS

S. No	Pattern	EMC	Simulation Parameter									
			Voltage(V)			Current(A)			Power(W)			
			Max	Min	Avg	Max	Min	Avg	Max	Min	Avg	OSC%
1	PT1	SMC-ANFIS	396.60	393.00	392.80	11.80	11.75	11.77	4531	4497	4514	1.93
2		SMC-ANN	390.50	374.80	382.65	12.10	11.53	11.89	4570	4658	4614	4.10
3		SMC	385.60	366.60	376.10	12.98	12.47	12.57	4826	4695	4760	5.00
1	PT2	SMC-ANFIS	396.30	396.80	396.60	12.05	11.68	11.86	4802	4694	4748	1.00
2		SMC-ANN	402.20	391.60	396.90	12.33	11.68	12.00	4944	4483	4713	2.60
3		SMC	398.80	385.70	392.25	12.48	11.25	11.86	5019	4401	4710	3.31
1	PT3	SMC-ANFIS	399.06	397.80	398.43	11.90	11.81	11.86	4772	4713	4742	0.5
2		SMC-ANN	401.30	398.50	399.90	11.98	11.87	11.95	4845	4734	4789	0.7
3		SMC	403.80	398.40	401.10	12.08	11.90	11.99	5001	4760	4880	1.3

TABLE VI. SIMULATION RESULT OF MECHANICAL PARAMETERS

S. No	Pattern	EMC	Torque		Speed (rpm)		
			Min	Max	Min	Max	Average
1	PT1	SMC-ANFIS	20.42	20.98	814.70	849.80	832.25
2		SMC-ANN	19.96	20.92	804.20	835.30	819.75
3		SMC	20.10	21.50	767.50	820.90	794.20
1	PT2	SMC-ANFIS	20.58	20.98	851.10	853.50	852.20
2		SMC-ANN	20.04	12.01	855.10	840.90	848.00
3		SMC	20.47	20.98	836.20	847.40	841.80
1	PT3	SMC-ANFIS	20.71	20.98	852.40	859.40	855.90
2		SMC-ANN	20.47	21.02	847.00	861.90	854.45
3		SMC	20.67	21.18	856.70	862.90	859.80

In PT3 configuration, the simulation carried out for the duration of 1.00s to 1.50s, the SMC-ANFIS controller supplies 8742 W power to the load and speed of the motor almost constant 855.90 rpm and the power oscillation is about 0.5%.

In case of SMC- ANN controller, the speed drops to 840 rpm and oscillation between 847 rpm and 861 rpm and power oscillation is 0.7%.

In the case of SMC-EMS, operational power is of 4880 W due to power oscillation between 5001 W to 4760 W and its oscillation nearly 1.3% and speed reduced to 833 rpm at dynamically change condition.

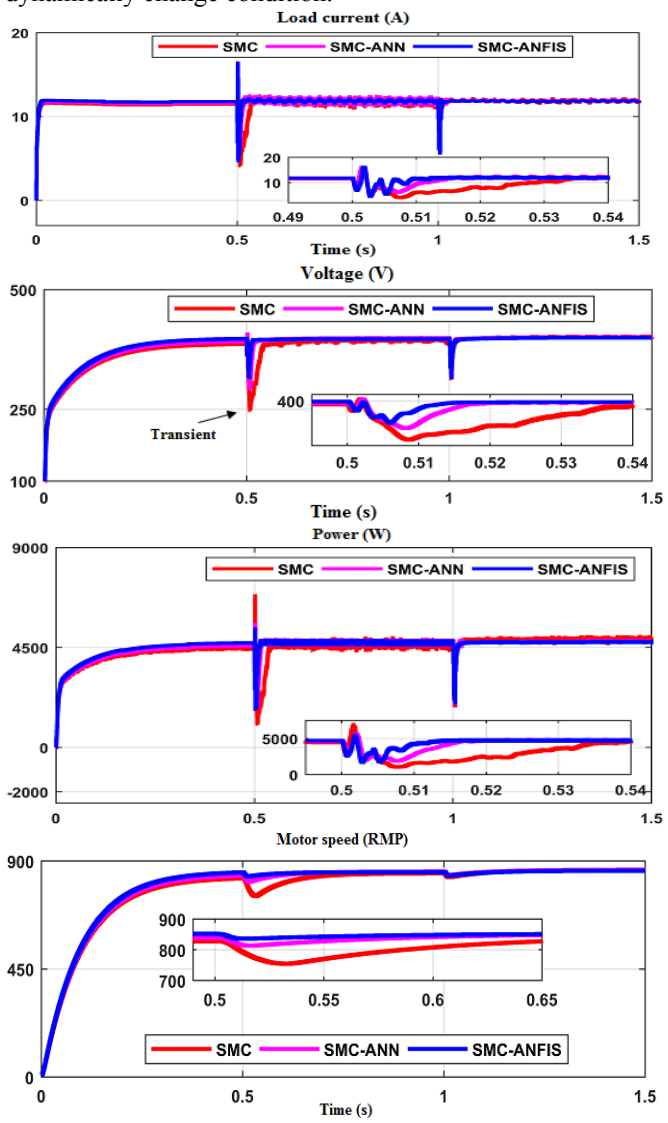

Figure 16. Comparison of load current, voltage, power and motor speed

VI. Experimental Validation

A scaled-down experimental prototype to validate the proposed idea has been constructed and tested. The specifications of the prototype developed are as follows. The experimental verification has been tested with a battery charging system consisting of 2 number of 12 V, 35 Ah batteries connected in series. The photograph of the proposed system is shown in Fig. 17. The ISSBC has been implemented in a general-purpose power electronic prototype kit where the power electronics are mounted with open terminals. The user can wire up the power electronic switches along with the external components. There is a provision of optical isolation of the control circuit and the power circuit. The IC MCT2E is used for optical isolation.

The prototype has an onboard PIC16F877A microcontroller. There is also a provision for attenuating the input and output voltages and currents. The microcontroller and the opto couplers are fed with DC power supplies derived from separate 230 V / 9 V transformers. The microcontroller is fed with a regulated 5 VDC power supply, and the opto coupler's DC supplies are not regulated. After wiring up the topology as per the specific application, the hex codes of the control program is developed in any C language programming environment. The important waveforms have been recorded and are presented in Fig. 18 and Fig. 19.

Figure 17. Hardware setup of SMC-ANFIS based EMS

TABLE VII. THE POWER BALANCE THROUGH THE SYSTEM OF POWER CONVERSION WHILE THE SOLAR IRRADIANCE IS 500 W/M^2

Subsystem	Output Terminal Voltage	Output Current	Power Delivered
SPV to ISBBC	16.7 V	3.76 A	62.8 W
ISBBC to Battery	22.2 V	2.35 A	53.58 W

TABLE VIII. THE POWER BALANCE THROUGH THE SYSTEM OF POWER CONVERSION WHILE THE SOLAR IRRADIANCE IS 950 W/M^2

Subsystem	Output Terminal Voltage	Output Current	Power Delivered
SPV to ISSBC	17.1 V	6.8 A	116.2 W
ISSBCto Battery	24.7 V	4.45 A	110 W

Fig. 18 shows the switching pulses applied to the MOSFET. These switching pulses areas dictated by the SMC algorithm embedded in the microcontroller PIC 16F877A. The switching pulses reach the gate of the MOSFET through the Opto Isolator IC MCT2E. The resulting current through the inductor L of the SCBBC and the voltage across the MOSFET are shown in Fig. 18 and Fig. 19.

VII. Conclusion

An intelligent control algorithm for power management in integrated Hybrid Energy System includes partial Shaded PV system and Fuel Cell to supply the standalone DC system has been developed. The Integrated Hybrid system is configured by different combination of renewable source and activation by the SMC-ANFIS control algorithm. The simulation result of proposed system is compared with conventional SMC and SMC-ANN EMS. In the Electrical parameter, the power oscillation for the entire three patterns got reduced by SMC-ANFIS.

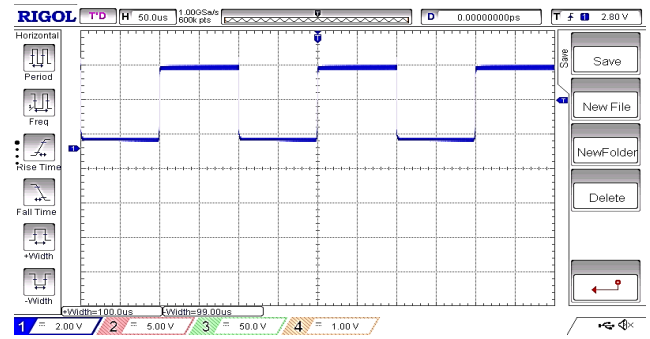

(a)

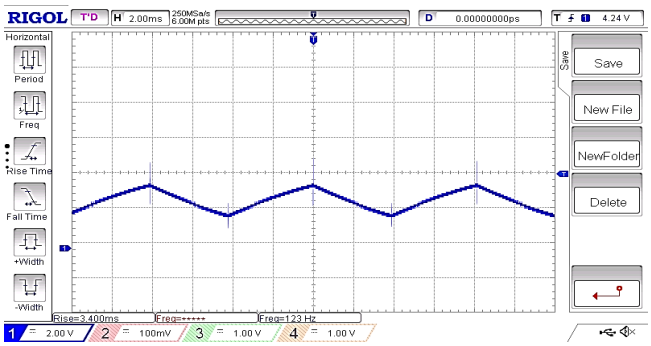

(b)

Figure 18. (a) The switching pulses applied to the MOSFET. (b) The current through the inductor

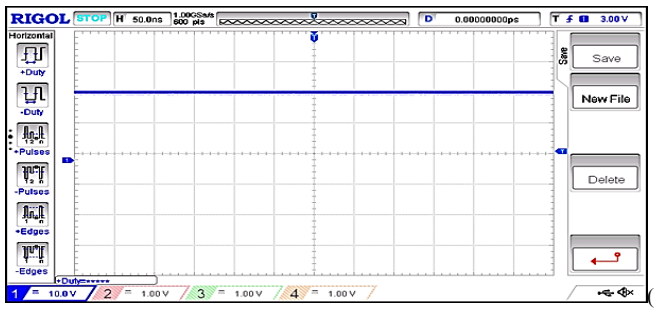

a)

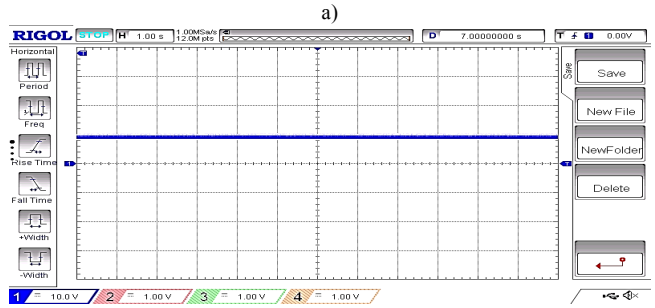

(b)

Figure 19. a) The terminal Voltage of the PV panel. (b) The voltage across the battery

In pattern (PT1) of SMC-ANFIS, the power oscillation reduced to 1.93% while other controller SMC and SMC-ANN got 5% and 4.1% correspondingly. In PT2, the SMC-ANFIS reduced the oscillation to 1% while other two reached 3.31% and 2.6%. In PT3, the SMC-ANFIS reduced the oscillation to 0.5% while other two reached 1.3% and 0.7%. Similarly in Mechanical parameters, the controller SMC-ANFIS produces the average speed of 832.25 rpm, 852.20 rpm and 855.9 rpm corresponding to PT1, PT2 and PT3 while other two controllers stuck. The proposed system with SMC-ANFIS controller has a better responsiveness, as evidenced by the extensive study of the simulated data when compared with other SMC and SMC-ANN controllers. Experimentation was also carried out, with the findings proving the correctness of the proposed concept.

REFERENCES

[1] S. Natarajan, F. Kamran, N. Ragavan, R. Rajesh, R. Jena, S. Suraparajua, "Analysis of PEM hydrogen fuel cell and solar PV cell hybrid model," Materials today proceeding, Vol. 17, no. 1, pp. 246-253, Jan. 2019. doi:10.1016/j.matpr.2019.06.426

[2] C. Ghenai, M. Bettayeb, "Grid-tied solar PV/fuel cell hybrid power system for university building," Energy Procedia, Vol. 159, pp. 96-103, Feb. 2019. doi:10.1016/j.egypro.2018.12.025

[3] N. S. Jayalakshmi, J. N. Sabhahit, D. N. Gaonkar, P. B. Nempu, "Integrated power flow and voltage regulation of stand-alone PV-fuel cell system with super capacitors," International Journal of Power and Energy Systems, vol. 37, no. 1, pp. 1-9, Aug. 2017. doi:10.2316/journal.203.2017.1.203-6251

[4] C. Ghenai, T. Salameh, A. Merabet, "Technico economic analysis of off grid solar PV/Fuel cell energy system for residential community in desert region," International Journal of Hydrogen Energy, vol. 45, no. 20, pp. 11460-11470, Apr. 2020. doi:10.1016/j.ijhydene.2018.05.110

[5] S. Rehman, Md. Mahbub Alam, J. P. Meyer, L. M. Al-Hadhrami, "Feasibility study of a wind/PV/diesel hybrid power system for a village," Renewable Energy, vol. 38, no. 1, pp. 258-268, Feb. 2012. doi:10.1016/j.ijhydene.2018.05.110

[6] J. Hivziefendic, L. Vuic, S. Lale, M. Saric, "Application of the voltage control technique and MPPT of stand-alone PV system with storage," Advances in Electrical and Computer Engineering, vol. 22, no. 1, pp 21-30, Feb. 2022. doi:10.4316/AECE.2022.01003

[7] A. Sfirat, A. Gontean, S. Bularka, "New method for MPPT algorithm implementation and testing, suitable for photovoltaic cells," Advances in Electrical and Computer Engineering, vol. 18, no.3, pp. 53-60, Aug. 2018. doi:10.4316/AECE.2018.03008

[8] M. Patterson, N. F. Macia, A. M. Kannan, "Hybrid micro grid model based on solar photovoltaic battery fuel cell system for intermittent load applications," IEEE Transactions on Energy Conversion, vol. 30, no. 1, pp. 359–366, Mar. 2015. doi:10.1109/TEC.2014.2352554

[9] P. Prabhakaran, V. Agarwal, "Novel four-port DC–DC converter for interfacing solar PV–fuel cell hybrid sources with low-voltage bipolar DC microgrids," IEEE Journal of Emerging and Selected Topics in Power Electronics, vol. 8, no. 2, pp. 1330–1340, Jun. 2020. doi:10.1109/JESTPE.2018.2885613

[10] S. M. Hakimi, A. Hasankhani, M. Shafie-khah, J. P. S. Catalao, "Optimal sizing and siting of smart microgrid components under high renewable penetration considering demand response," IET Renewable Power Generation, vol. 13, no. 10, pp. 1809–1822, Jul. 2019. doi:10.1049/iet-rpg.2018.6015

[11] P. B. Nempu, N. S. Jayalakshmi, "Stochastic algorithms for controller optimization of grid tied hybrid AC/DC microgrid with multiple renewable sources," Advances in Electrical and Computer Engineering, vol. 19, no. 2, pp. 53-60, Jan. 2019. doi:10.4316/AECE.2019.02007

[12] F. Cingoz, A. Elrayyah, Y. Sozer, "Optimized resource management for PV–fuel-cell-based microgrids using load characterizations," IEEE Transactions on Industry Applications, vol. 52, no. 2, pp. 1723–1735, Mar 2016. doi:10.1109/TIA.2015.2499287

[13] P. Thounthong, A. Luksanasakul, P. Koseeyaporn, B. Davat, "Intelligent model-based control of a standalone photovoltaic/fuel cell power plant with supercapacitor energy storage," IEEE Transactions on Sustainable Energy, vol. 4, no. 1, pp. 240-249, Jan 2013. doi:10.1109/TSTE.2012.2214794

[14] R. Sharma, S. Mishra, "Dynamic power management and control of a PV PEM fuel-cell-based Standalone AC/DC microgrid using hybrid energy storage," IEEE Transactions on Industry Applications, vol. 54, no. 1, pp. 526–538, Jan. 2018. doi:10.1109/TIA.2017.2756032

[15] U. Raveendran Nair, R. Costa Castello, "A model predictive control-based energy management scheme for hybrid storage system in islanded microgrids," IEEE, vol. 8, pp. 97809–97822, May. 2020. doi:10.1109/ACCESS.2020.2996434

[16] S. Babu, L. Ashok Kumar, "Voltage controller with energy management unit for microgrid with hybrid sources," Energy Exploration & Exploitation, vol. 39, no. 3, pp. 1–24, Jun. 2021. doi:10.1177/01445987211015392

[17] V. Dash, P. Bajpai, "Power management control strategy for a stand-alone solar photovoltaic-fuel cell–battery hybrid system," Sustainable Energy Technologies and Assessments, vol. 9, no. 1, pp. 68–80, Mar. 2015. doi:10.1016/j.seta.2014.10.001

[18] A. Vinayagam, A. Alqumsana, K. S. V. Swarnaa, S. Yang Khooa, "Intelligent control strategy in the islanded network of a solar PV microgrid," Electric Power Systems Research, vol. 155, pp. 93–103, Feb. 2018. doi:10.1016/j.epsr.2017.10.006

[19] P. Nammalvar, S. Ramkumar, "Parameters improved particle Swarm optimization based direct-current vector control strategy for solar PV system," Advances in Electrical and Computer Engineering, vol. 18, no. 1, pp. 105–112, Feb. 2018. doi:10.4316/AECE.2018.01013

[20] A. Elgammal, M. F. El- Nagger, "Energy management in smart grids for the integration of hybrid wind PV/ FC/ battery renewable energy resources using multi-objective particle swarm optimization," The Journal of Engineering, vol. 2018, no. 11, pp. 1806–1816, Sep. 2018. doi:10.1049/joe.2018.5036

[21] A. M. Noman, K. E. Addoweesh, A. I. Alolah, "Simulation and practical implementation of ANFIS-based MPPT method for PV applications using isolated ćuk converter," Hindawi, International Journal of Photoenergy, vol. 2017, no. 1, pp. 1-15, Dec. 2017. doi:10.1155/2017/3106734

[22] A. Afsin Kulaksiz, "ANFIS-based estimation of PV module equivalent parameters: application to a stand-alone PV system with MPPT controller," Turkish Journal of Electrical Engineering & Computer Sciences, vol. 21, pp. 2127-2140, Jan. 2013. doi:10.3906/elk-1201-41

[23] M. Jafari, Z. Malekjamshidi, D. Dah-Chuan Lu, J. Zhu, "Development of a fuzzy-logic-based energy management system for a multiport multioperation mode residential smart microgrid," IEEE Transactions on Power Electronics, vol. 34, no. 4, pp. 3283–3301, Apr. 2019. doi:10.1109/TPEL.2018.2850852

[24] S. Nascimento, M. M. Gouvêa Jr., "Multi-objective adaptive evolutionary algorithm to enhance voltage stability in power systems," International Journal of Control, Automation, and Systems, vol. 19, no. 7, pp. 2596-2610, May, 2021. doi:10.1007/s12555-020-0095-4

[25] Y. K. Renani. B. Vahidi, H. A. Abyaneh, "Effects of photovoltaic and fuel cell hybrid system on distribution network considering the voltage limits," Advances in Electrical and Computer Engineering, vol. 10, no. 4, pp. 143-148, Nov. 2010. doi:10.4316/aece.2010.04023